Improved performance of near UV light-emitting diodes with a composition-graded p-AlGaN irregular sawtooth electron-blocking layer*

Ping Qin(秦萍)[1], Wei-Dong Song(宋伟东)[1], Wen-Xiao Hu(胡文晓)[1], Yuan-Wen Zhang(张苑文)[1], Chong-Zhen Zhang(张崇臻)[1], Ru-Peng Wang(王汝鹏)[1], Liang-Liang Zhao(赵亮亮)[1], Chao Xia(夏超)[1], Song-Yang Yuan(袁松洋)[1], Yi-an Yin(尹以安)[1,2], Shu-Ti Li(李述体)[1,2], and Shi-Chen Su(宿世臣)[1,2,†]

[1] *Guangdong Provincial Key Laboratory of Nanophotonic Functional Materials and Devices, Institute of Opto-electronic Materials and Technology, South China Normal University, Guangzhou* 510631, *China*

[2] *Guangdong Engineering Research Center of Optoelectronic Functional Materials and Devices, Institute of Opto-electronic Materials and Technology, Guangzhou* 510631, *China*

(Received 27 January 2016; revised manuscript received 8 April 2016; published online 25 June 2016)

We investigate the performances of the near-ultraviolet (about 350 nm–360 nm) light-emitting diodes (LEDs) each with specifically designed irregular sawtooth electron blocking layer (EBL) by using the APSYS simulation program. The internal quantum efficiencies (IQEs), light output powers, carrier concentrations in the quantum wells, energy-band diagrams, and electrostatic fields are analyzed carefully. The results indicate that the LEDs with composition-graded p-$Al_xGa_{1-x}N$ irregular sawtooth EBLs have better performances than their counterparts with stationary component p-AlGaN EBLs. The improvements can be attributed to the improved polarization field in EBL and active region as well as the alleviation of band bending in the EBL/p-AlGaN interface, which results in less electron leakage and better hole injection efficiency, thus reducing efficiency droop and enhancing the radiative recombination rate.

Keywords: AlGaN-based ultraviolet LEDs, irregular sawtooth EBL, APSYS simulation program, output power

PACS: 85.60.Jb, 73.40.Kp, 78.20.Bh, 87.16.ad **DOI:** 10.1088/1674-1056/25/8/088505

1. Introduction

It is more and more important to improve the quality of AlGaN layers through optimizing structure designs in group III-nitride-based ultraviolet (UV) light-emitting diodes (LEDs) for their wide applications in the fields such as air and water purification, automobile exhaust purifiers, surface disinfection, UV curing and medical phototherapy, etc.[1–3] In recent years, AlGaN-based ultraviolet (UV) light-emitting diodes (LEDs) have made significant progress.[4–7] Hideki *et al*. fabricated a UV-LED with quaternary InAlGaN multiple-quantum-well (MQW) and realized a maximum output power of 7.4 mW and an emission wavelength of 352 nm under room temperature (CW) operation.[8] Yang *et al*. proposed a novel AlGaN-based LED with a specific design by using staggered AlGaN quantum wells, and thus effectively improving the electron and hole wave function overlap.[9] AlGaN-based near-UV light-emitting diode (350 nm–360 nm) with an output power as high as 9.8 mW at 40 mA was achieved on a low-dislocation-density AlGaN/sapphire template via a single growth step in situ SiNx interlayer technic.[10] Ma *et al*. designed an AlGaInP-based LED with a 0.5-μm GaP window layer, and also used indium tin oxide (ITO) and localized Cr deposition as the current spreading layer and the Schottky current blocking layer (CBL) beneath the p-pad electrode. The experimental result shows that the light output power can be improved by 40%.[11] However, further studies are still necessary on near-UV light-emitting diodes (LEDs) for high-brightness and high-power applications. Previous reports have proposed various possible mechanisms for the low-efficiency, electron overflow out of the active region, nonuniform distributions of holes and electrons, poor crystalline quality, and poor hole injection.[12–15] Among these factors, the electron leakage from multi-quantum wells (MQWs) into the p-type layers and the low hole-injection efficiency have been discussed intensively. Conventionally, it can be used to suppress the electrons overflowing though a p-AlGaN electron blocking layer (EBL) with high Al content. However, inevitably, the insert of a layer of a typical EBL is supposed to cause band bending at the interface and reduce blocking efficency, resulting from the severe lattice mismatch induced polarization fields.[16–18] At the same time, the polarization-field induced band bending and the valence band offset at

*Project supported by the National Natural Science Foundation of China (Grant Nos. 11474105 and 51172079), the Science and Technology Program of Guangdong Province, China (Grant Nos. 2015B090903078 and 2015B010105011), the Program for Changjiang Scholars and Innovative Research Team in University, China (Grant No. IRT13064), the Science and Technology Project of Guangzhou City, China (Grant No. 201607010246), and the Science and Technology Planning Project of Guangdong Province, China (Grant No. 2015A010105025).

†Corresponding author. E-mail: shichensu@126.com

© 2016 Chinese Physical Society and IOP Publishing Ltd

the interface of p-AlGaN and EBL are thought to impede the injection of holes.[19] Therefore, a conventional EBL with high Al content is not enough for high-efficiency UV-LED, and more complicated and optimized EBL design is needed. Many structure designs with respect to EBL have been brought up, like AlGaN-based deep UV-LEDs with AlN/AlGaN or AlGaN/AlGaN multiquantum-barrier (MQB) EBL,[20] composition-graded EBL,[21,22] near-UV LEDs with InAlN/GaN superlattice EBL,[23] etc. In their designs, problems related to the effective barrier height of EBL, holes transportation across the EBL and electrons confinement have been addressed appropriately. In this work, we design and theoretically study near-UV light-emitting diodes (350 nm–360 nm) each with a composition-graded p-$Al_xGa_{1-x}N$ irregular sawtooth EBL with the Advanced Physical Models of Semiconductor Devices simulation (APSYS) program. We aim to provide more documents about novel and optimized EBL structure designs for high-efficiency near-UV LED applications. The results show that the LEDs with the irregular sawtooth EBL exhibit much higher output power and internal quantum efficiency compared with those with stationary component EBL due to the less electron leakage and improvement of the hole injection from the p-type region.

2. LED structures and simulation parameters

The structure of AlGaN based MQWs UV-LED with a stationary component AlGaN EBL (denoted as structure A) as shown in Fig. 1, is used as a reference in this study. Both the reference and the modified structures were fabricated on *c*-plane sapphire substrates using metal organic chemical vapor deposition (MOCVD). Both devices included a 3.0-μm-thick n-$Al_{0.15}Ga_{0.85}N$ layer (n-doping $= 2\times10^{18}$ cm^{-3}), followed by active layers consisting of five 30-Å-thick GaN wells separated by 100-Å-thick $Al_{0.15}Ga_{0.85}N$ barriers. All wells and barrier layers were undoped. The fabricated reference LED consisted of a 22-nm-thick p-$Al_{0.3}Ga_{0.7}N$ EBL (p-doping $= 1\times10^{17}$ cm^{-3}) and a 20-nm-thick p-$Al_{0.15}Ga_{0.85}N$ layer (p-doping $= 1\times10^{17}$ cm^{-3}) on top of the active region, followed by an 80-nm-thick p-GaN cap layer (p-doping $= 1\times10^{18}$ cm^{-3}). For the modified structure, a specifically designed irregular sawtooth electron blocking layer (EBL) was designed. The schematic diagrams of the structures are shown in Fig. 1. The detailed design of the irregular sawtooth EBL was as follows: (i) a 5.0-nm-thick p-AlGaN (p-doping $= 1\times10^{17}$ cm^{-3}) with the Al content decreasing from 0.3 to 0.1 was grown at first; (ii) in the middle of the EBL, two pairs of sawtooth AlGaN layers (p-doping $= 1\times10^{17}$ cm^{-3}) containing a linear increasing part (Al content: from 0.1 to 0.2) and a linear decreasing part (Al content: from 0.2 to 0.1) were used; the thickness of each composition-graded p-AlGaN layer was set to be 3.0 nm; (iii) finally, a 5.0-nm-thick p-AlGaN (p-doping $= 1\times10^{17}$ cm^{-3}) with the Al content increasing from 0.1 to 0.3 was adopted. The device geometry was designed into a rectangular shape of 200 μm×200 μm. In the carrier recombination model, the Schockley–Read–Hall (SRH) recombination lifetime was assumed to be 5 ns and the internal loss was 1000 m^{-1}.[24] The Auger recombination coefficient was set to be 1×10^{-30} cm^6/s[25] and the operating temperature was assumed to be 300 K. The built-in interface polarization charges due to the spontaneous and piezoelectric polarization were calculated based on the methods proposed by Fiorentini *et al.*[26] In order to consider the built-in polarization within the interface, the spontaneous polarization of $Al_xGa_{1-x}N$ alloys can be expressed as

$$P_{sp}(Al_xGa_{1-x}N) = -0.090x - 0.034(1-x) + 0.019x(1-x).$$

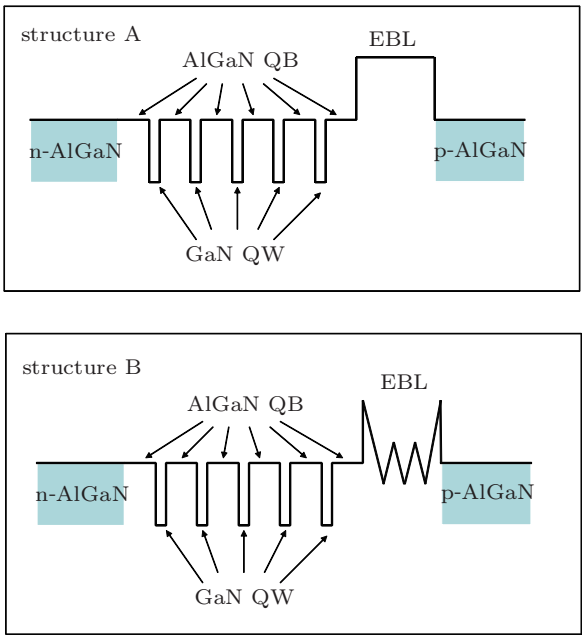


Fig. 1. (color online) Schematic diagrams of structures A and B.

On the other hand, the piezoelectric polarization of $Al_xGa_{1-x}N$ can be calculated from the following expression: $P_{pz}(Al_xGa_{1-x}N) = P_{pz}(AlN)x + P_{pz}(GaN)(1-x)$, where

$$P_{pz}(AlN) = -1.808\varepsilon + 5.624\varepsilon^2, \quad \text{for} \quad \varepsilon < 0,$$
$$P_{pz}(AlN) = -1.808\varepsilon - 7.888\varepsilon^2, \quad \text{for} \quad \varepsilon > 0,$$
$$P_{pz}(GaN) = -0.918\varepsilon + 9.541\varepsilon^2.$$

The discussed basal strain function is

$$\varepsilon(x) = [a_{subs} - a(x)]/a(x),$$

with $a(x)$ and a_{subs} being the lattice constants of the unstrained alloy at composition x, and of the substrate (assumed to be noncompliant) respectively. In the case of pseudomorphic

growth, basal strain ε can be calculated directly from the lattice constants, which are found to follow Vegard's law as a function of composition:
$a_{Al_xGa_{1-x}N}(x) = 0.31986 - 0.00891x$.[26]
Then the net polarization charge at the $Al_xGa_{1-x}N/Al_yGa_{1-y}N$ heterointerface is

$$\sigma_{Al_xGa_{1-x}N/Al_yGa_{1-y}N} = (P^{sp}_{Al_yGa_{1-y}N} + P^{pz}_{Al_yGa_{1-y}N}) - (P^{sp}_{Al_xGa_{1-x}N} + P^{pz}_{Al_xGa_{1-x}N}).$$

Furthermore, concerning the screening by defects, the surface charge densities are assumed to be 40% of the calculated values.[27] More detailed material parameters of semiconductors used in this simulation can be found in Ref. [28].

3. Results and discussion

Figure 2 shows the energy-band diagrams and quasi-Fermi levels of the two structures at 450 A/cm^2. It can be seen that the effective barrier height for electron in structure A is 275 meV, lower than that of structure B (318 meV). Relatively, the effective hole barrier heights for structure A and structure B are 235 meV and 233 meV, respectively. It is worth noting that for structure A, the spontaneous polarization fields induced by larger lattice mismatch that is caused by the relatively high Al composition in EBL have pulled down the energy band at the interfaces of the last quantum barrier/EBL and the EBL/p-AlGaN. So both the conduction band bending and the valence band bending are very serious, which results in potential wells at the interface as shown by the arrows in Fig. 2(a). In the conduction band, this potential well is below the electron quasi-Fermi level and thus a lot of electrons can be accumulated at the interface between the last quantum barrier and p-AlGaN EBL. Besides, due to the band banding, the effective barrier height of EBL for electron decreases so that severe electron overflow could be expected. As for the valence band, it is apparent that the potential well at the interface between the EBL and p-AlGaN can also accumulate the holes, which increases difficulties for the holes to transport across the EBL. However, the structure B with a p-$Al_xGa_{1-x}N$ irregular sawtooth EBL can reduce the polarization effect and modify the position of EBL's band edge relative to quasi-Fermi level. As a result, the band-bending at the interface near the EBL is alleviated and the negative accumulation of the carriers decreases significantly. Thus, the hole-injection efficiency can be increased effectively. At the same time, the EBL has a relatively high effective barrier height for electron transportation so that electron leakage from QW to p-type layer can be commendably prevented. Considering the electron blocking effect and the hole-injection efficiency, structure B has much better advantages than structure A.

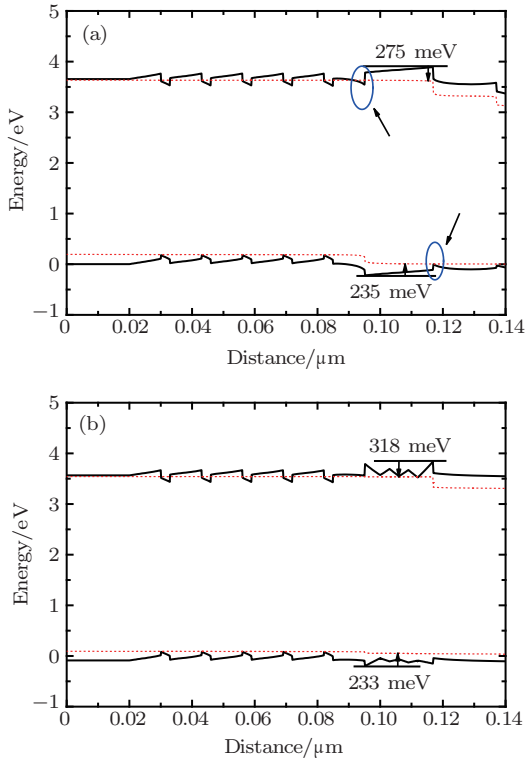


Fig. 2. (color online) Energy-band diagrams of (a) structure A and (b) structure B, at 180 A/cm^2.

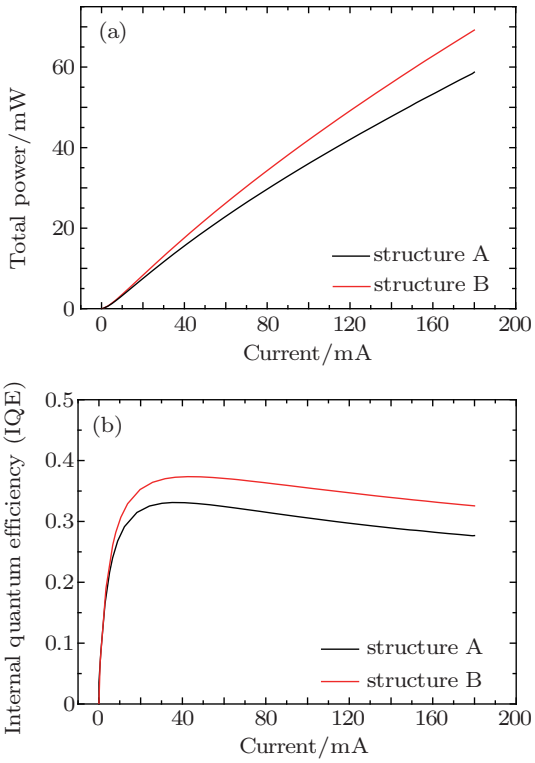


Fig. 3. (color online) (a) Total powers versus current of structures A and B. (b) Simulation results of internal quantum efficiency (IQE) versus current for structures A and B.

To study the advantages of the modified near UV-LED structure with irregular sawtooth EBL, the performances of optical power and the IQE of both structures are investigated. Figure 3(a) shows the typical *P–I* characteristics of these two different near-UV LED structures. The light output power of

structure A at 180 mA is 58 mW, much higher than that of structure B (70 mW) under the same condition. The reason for this is considered to be the improved carrier density in QW for the modified EBL in structure B, owing to the relatively high potential barrier height and the improved band bending in the conduction band and valence band. The internal quantum efficiencies (IQEs) each as a function of the inject current for both structures are simulated (see Fig. 3(b)). As forward current increases, the IQEs of the two LED structures show similar variation trends. But it can be seen that the IQE performance of structure B is much better than that of structure A. At the peak value position, the IQE of structure B is 13.8% higher than that of structure A. On the other hand, as the current increases to 180 mA, the efficiency droops of structure A and structure B are 20% and 14.8%, respectively. This indicates that the efficiency droop is improved significantly under high current in structure B. This can be attributed to the improved hole injection efficiency and electron blocking efficiency in our specially designed irregular sawtooth EBL for the near-UV LEDs.

In order to better understand the above results, the electron current density distribution near the active region is calculated. Figure 4(a) shows the electron current versus distance at the MQWs, EBL, and p-AlGaN layer in the vertical direction when the current density is 450 A/cm^2. Electron current at the right-most side of the figure corresponds to the electron leakage current, which is defined by the electron current overflowing from the active region to the p-type layers. Electron leakage is another important factor influencing the light efficiency. It can be seen that almost 17.5% of the injected electron current of structure A has leaked to the p-AlGaN when the current density is 450 A/cm^2. However, the electron leakage of structure B has reduced to 5.0% at 450 A/cm^2, much lower than that of structure A. This means that more electrons in structure B are confined and participated in the process of radiative recombination, which results in higher internal quantum efficiency. We propose that our novel design of irregular sawtooth EBL could effectively reduce the lattice mismatch between the last quantum barrier and the EBL, thus alleviating the polarization field induced band bending. The simulated carrier concentrations of the two structures in MQWs cut from n-side to p-side at 180 mA are plotted in Figs. 4(b) and 4(c). Note that the horizontal position of structure A is shifted slightly for better observation. Both the hole-concentration and electron-concentration in MQWs with an irregular sawtooth EBL are higher than the conventional ones and are distributed uniformly, which means that the hole-carrier injection into the MQWs is enhanced efficiently. But for the conventional structure, due to the serious conduction and valence band bending, two relatively deep potential wells are formed at the interfaces of MQWs and EBL (as shown by the arrow in Fig. 2(a)), inevitably leading to more electrons and holes accumulated at the interfaces. It can be seen from Figs. 4(b) and 4(c) that the hole concentration and electron concentration at interfaces are much higher, which is highly related to the nonradiative loss of carriers. It is worth mentioning that certain concentrations of electron and hole are distributed in the sawtooth EBL, but they are much lower than those of the conventional structure. So the use of an irregular sawtooth EBL still has a better performance.

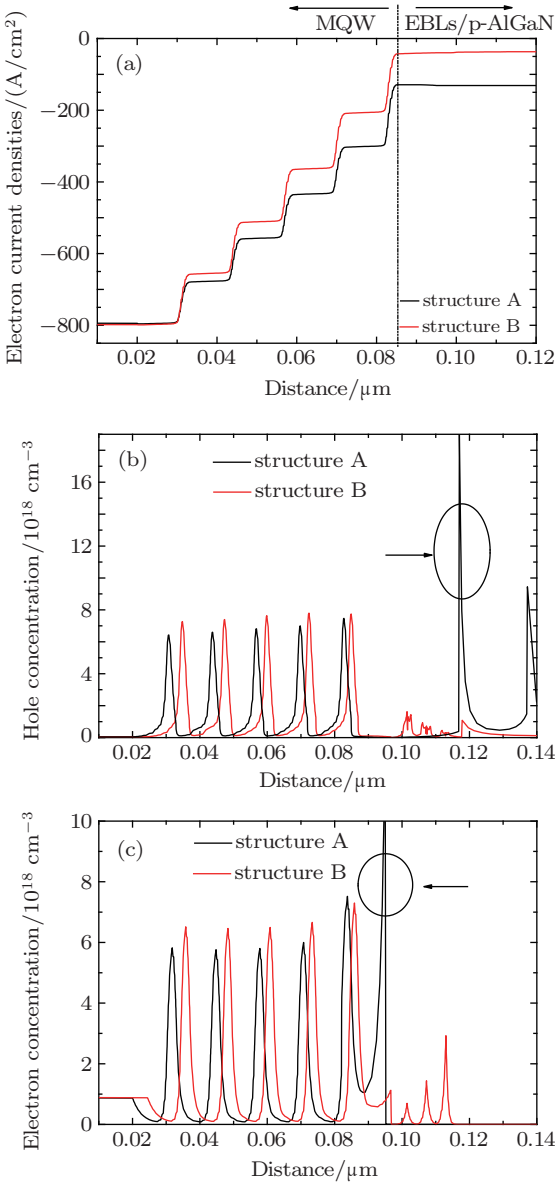


Fig. 4. (color online) (a) Electron current densities versus distance of structures A and B; (b) and (c) hole concentration and electron concentration versus distance of structures A and B at 180 mA.

Figure 5 shows the radiative recombination rate and spontaneous emission rates of both LED structures at 450 A/cm^2. For the radioactive recombination rates, the horizontal position of structure A has been shifted slightly for better observation. The result shows that structure B has a higher radiative recombination rate than structure A. This phenomenon can be explained by the rational structure design. The potential well at the interface (as shown by the arrow in Fig. 2(a)) in

structure A is ameliorated effectively by our optimized structure with an irregular sawtooth EBL. Due to the enhancements of electron confinement and hole injection efficiency, more carriers are confined in MQWs with irregular sawtooth EBL. Thus, the radiative recombination rate of structure B is higher than that of structure A. This is consistent with our results observed above that the structure B has better optical and electrical performances such as improved light output power, higher internal quantum efficiency, and smaller leakage current. In addition, as plotted in Fig. 5(b), the spontaneous emission rate of structure B is much higher than that of structure A at 180 mA, which is ascribed to its enhanced radiative recombination rate. It is worth noting that certain concentrations of electrons and holes are distributed in the sawtooth EBL as shown in Figs. 4(b) and 4(c), which may produce a corresponding photoluminescence peak. But it can be found that both of these two structures are single-peaked operation and the emission peak wavelength is 352 nm at 450 A/cm^2, indicating that there is no additional radiative emission happening in the irregular sawtooth EBL. Of course, actual device luminescence performance still needs further studying.

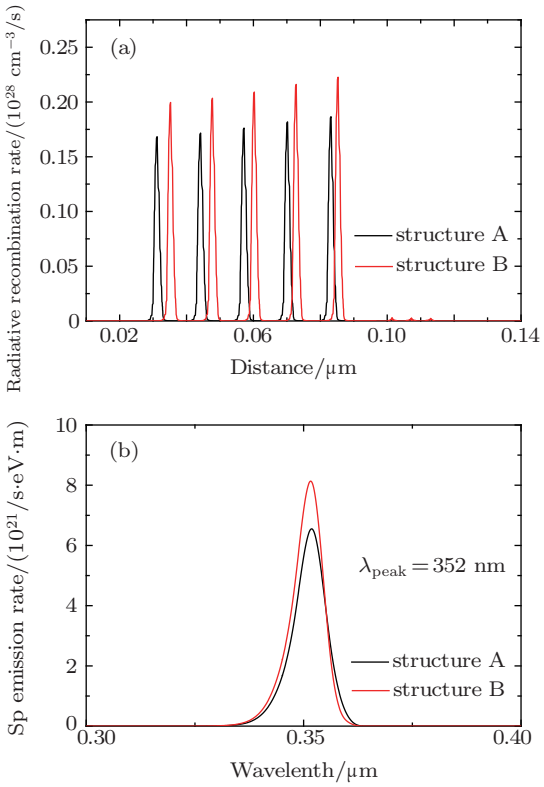


Fig. 5. (color online) The (a) radiative recombination rates versus distance and (b) spontaneous (SP) emission rates versus wavelength for structures A and B at 180 mA.

4. Conclusions

The advantages of AlGaN/GaN based near-UV-LED with an irregular sawtooth EBL are investigated numerically. The results show that the optical power of the structure with irregular sawtooth EBL is improved by 20.7% and the IQE efficiency droop is reduced by 26% under an injection current of 180 mA in comparison with the conventional LED with a stationary component p-AlGaN EBL. The reason is that this modified structure has an improved polarization field at the interface and thus the conduction band bending and valence band bending are alleviated effectively, which results in less electron leakage and better hole injection efficiency. Furthermore, the specially designed EBL has a relatively high effective barrier for electrons to transport due to the relaxed band-bending, so that electrons can be confined in MQW effectively.

References

[1] Asif K, Krishnan B and Tom K 2008 *Nat. Photon.* **2** 77
[2] Li, J, Lin J Y and Jiang H X 2006 *Appl. Phys. Lett.* **88** 171909
[3] Yu H P, Li S B, Zhang P, Wu S H, Wei X B, Wu Z M and Chen Z 2014 *Chin. Phys. Lett.* **31** 108502
[4] Lu T P, Li S T, Zhang K, Liu C, Xiao G W, Zhou Y G, Zheng S W, Yin Y A, Wu L J, Wang H L and Yang X D 2011 *Chin. Phys. B* **20** 098503
[5] Yin Y A, Wang N Y, Fan G H and Zhang Z H 2014 *Superlattices Microstruct.* **76** 149
[6] Wu T, Feng Z H, Liu B, Xiong H, Zhang J B, Dai J N, Cai S J and Chen C Q 2013 *Opt. Quantum Electron.* **45** 381
[7] Cyril P, Shinya, Tetsuhiko I, Takehiko F, Myunghee K, Yosuke N, Akira H, Masamichi I, Motoaki I, Satoshi K, Isamu A and Hiroshi A 2011 *Phys. Stat. Sol. A* **208** 1594
[8] Hideki H, Katsushi A, Takashi K, Takao N and Koji I 2004 *J. Appl. Phys.* **43** L1241
[9] Yang G F, Xie F, Dong K X, Chen P, Xue J J, Zhi T, Tao T, Liu B, Xie Z L, Xiu X Q, Han P, Shi Y, Zhang R and Zheng Y D 2014 *Physica E* **62** 55
[10] Gutt R, Passow T, Kunzer M, Pletschen W, Kirste L, Forghani K, Scholz F, Köhler K and Wagner J 2012 *Appl. Phys. Express* **5** 032101 1882
[11] Ma L, Shen G D, Gao Z Y and Xu C 2015 *Chin. Phys. B* **24** 097202
[12] Kenneth J V, Michael I, Stacia K, Steven P D and Shuji N 2009 *Appl. Phys. Lett.* **94** 061116
[13] Wang C H, Chen J R, Chiu C H, Kuo H C, Li Y L, Lu T C and Wang S C 2010 *IEEE Photon. Technol. Lett.* **22** 236
[14] Aurélien D and Michael J G 2010 *Appl. Phys. Lett.* **96** 103504
[15] Monemar B and Sernelius B E 2007 *Appl. Phys. Lett.* **91** 181103
[16] Han S H, Lee D Y, Lee S J, Cho C Y, Kwon M K, Lee S P, Noh D Y, Kim D J, Kim Y C and Park S J 2009 *Appl. Phys. Lett.* **94** 231123
[17] Kuo Y K, Chang J Y, Tsai M C and Yen S H 2009 *Appl. Phys. Lett.* **95** 011116
[18] Xia, C S, Li Z M S, Lu W, Zhang Z H, Sheng Y, Hu W D and Cheng L W 2012 *J. Appl. Phys.* **111** 094503
[19] Jun Z, Wu T, Feng W, Weiyi Y, Hui X, Jiangnan D, Yanyan F, Zhihao W and Changqing C 2013 *IEEE Photon. J.* **5** 1600310
[20] Hirayama H, Tsukada Y, Maeda T and Kamata N 2010 *Appl. Phys. Express* **3** 031002
[21] Kuo Y K, Chang J Y and Tsai M C 2010 *Opt. Lett.* **35** 3285
[22] Yen S H and Kuo Y K 2008 *J. Appl. Phys.* **103** 103115
[23] Zhang Y Y, Zhu X L, Yin Y A and Ma J 2012 *IEEE Electron Dev. Lett.* **33** 994
[24] Yen S H and Kuo Y K 2008 *J. Appl. Phys.* **103** 103115
[25] Xia C S, Simon Li Z M, Li Z Q and Sheng Y 2013 *Appl. Phys. Lett.* **102** 013507
[26] Fiorentini V, Bernardini F and Ambacher O 2002 *Appl. Phys. Lett.* **80** 1204
[27] Chichibu S F, Abare A C, Minsky M S, Keller S, Fleischer S B, Bowers J E, Hu E, Mishra U K, Coldren L A, DenBaars S P and Sota T 1998 *Appl. Phys. Lett.* **73** 2006
[28] Vurgaftman I, Meyer J R and Ram-Mohan L R 2001 *J. Appl. Phys.* **89** 5815